

Simulation Modeling of Hydrothermal Energy Extraction with Two-layer Multilateral Horizontal wells

Guofeng Song, Xianzhi Song*, Gengsheng Li, Yu Shi, Gaosheng Wang

State Key Laboratory of Petroleum Resources and Prospecting, China University of Petroleum, Beijing, Beijing
102249, China

E-mail address, songxz@cup.edu.cn, 15650797007@163.com

Keywords: Hydrothermal energy, Multilateral horizontal wells, Numerical simulation, Heat extraction, Performance evaluation.

ABSTRACT

Geothermal energy is clean and sustainable as an alternative to fossil energy. Hydrothermal resources are one of the most important geothermal resources in the world. A two-layer multilateral horizontal well system is proposed to exploit hydrothermal energy with circulating groundwater in this paper. One main wellbore is drilled into the geothermal reservoir. Then several injection and production multilateral horizontal wells are side-tracked from the main wellbore in the upper and lower formation, respectively. In addition, a central insulation tube is installed in the main wellbore. Low-temperature water is injected into the geothermal reservoir through the main borehole annulus and then the injection laterals, to extract heat from the reservoir. Finally, the hot water is produced from the production laterals and pumped to the ground through the central insulated pipe, to be used for residential heating and power generation. In this paper, a three-dimensional unsteady fluid flow and heat transfer model is established for the two-layer multilateral horizontal well hydrothermal geothermal system. Four typical parameters, which are average production temperature, average pressure on injection wells, average production rate and net heat power, are defined and analyzed to evaluate the extraction performance of the system. The whole development can be divided into the stable production stage and the reduction stage based on the variation trend of four characteristic parameters. Moreover, the temperature field, pressure field and velocity field of the formation at different times are compared and investigated to describe visually the dynamic change of the hydrothermal system. As a result, the low temperature region expands like a funnel and the high pressure region shows like a sphere. This paper provides a novel and efficient two-layer multilateral horizontal well system and reveals the production characteristics of the system for the exploitation of hydrothermal resources.

1. INTRODUCTION

With the consumption of oil and natural gas resources, new energy sources including geothermal energy, solar energy and wind energy are gaining more and more attention. Geothermal energy is environmentally friendly and sustainable as an alternative to fossil energy. Compared with wind energy and solar energy, geothermal energy is not subjected to seasonal and weather restrictions. Additionally, geothermal energy is stable, low-carbon and has high capacity factor over 90% in many cases (Sims, 2014).

According to the global average terrestrial heat flow value, it is estimated that the dissipated heat, which transmitted from the Earth's interior to the surface every day, is equivalent to 2.5 times of the average daily energy used by human beings today (Wang et al., 1990). The abundant geothermal energy has great potential in residential heating and power generation. According to thermal storage conditions and thermal fluid transport, geothermal resources can be divided into shallow geothermal energy resources, hydrothermal resources and hot-dry-rock (HDR) geothermal resources. Shallow geothermal resources with low temperature are widely distributed within 100 meters underground. Hydrothermal geothermal resources (generally with 90-150 °C) are mainly distributed near faults or in areas with volcanoes and high-heat fluids nearby. The heat source of the hydrothermal reservoir is derived from the decay of radioactive elements in deep magma and granite. The reservoir is rich in natural fractures which provide the flowing channels with high permeability for the meteoric water or groundwater forming a relatively stable convective geothermal system (Lin et al., 2013). High-temperature hydrothermal geothermal areas have great potential for power generation. The temperature reaches 195°C at the depth of 230 m in the Gudui high temperature geothermal area in Cuomei of Tibet in the southwest region of China. The potential for generating electricity is up to 110 MW (Wang et al., 2018). The majority of geothermal energy is stored in hot dry rocks (normally mass matrix temperature at 150-650 °C) with little fluid and low permeability within the subsurface at 3-10 km depths (Panel, 2006). The concept of Enhanced Geothermal System (EGS) was proposed to exploit the huge potential of dry hot rocks. In conventional EGS, artificial methods (hydraulic fracturing, thermal stress, chemical and explosion, etc.) are applied to produce artificial cracks in HDR formations with low porosity and low permeability. Low-temperature working fluids are injected and hot fluids are produced from production wells for electricity generation. However, it is not easy to build a high-yield EGS project due to the enormous construction cost. In recent years, only the French Soultz EGS project has barely reached the economic level (André et al., 2006). The cost of drilling and completion of the EGS project with a depth of more than 5000 m is as high as 13 million dollars accounting for more than 50% of the total development cost (Lukowski et al., 2016).

Hydrothermal resources are usually distributed within no more than 4,000 meters underground which is shallower than HDR. Besides, a large number of natural cracks and abundant subsurface hot water in a high hydrothermal resources make it efficient to be used directly or for power generation at relatively low cost. Nowadays, two vertical or directional wells are drilled as injection and production wells in conventional hydrothermal geothermal system. One well is injected with cold water and the other one produces hot water. However, the control area of the vertical well is limited with low heat efficiency. In the end, the heat of the reservoir energy cannot be fully utilized. Han et al. (2016) proposed new heat pumps and Shi et al. (2018) investigated downhole heat exchangers to extract heat from low- and medium-temperature geothermal resources. These non-water production technologies with low cost provide new methods to solve the problems of insufficient groundwater recharge. The heat absorption range is limited to the vicinity

of the wellbore so far. Song et al. (2018) proposed a multilateral EGS system to exploit HDR and concluded that the heat extraction performance of multilateral-well EGS was equal to or even better than that of the conventional two-well EGS.

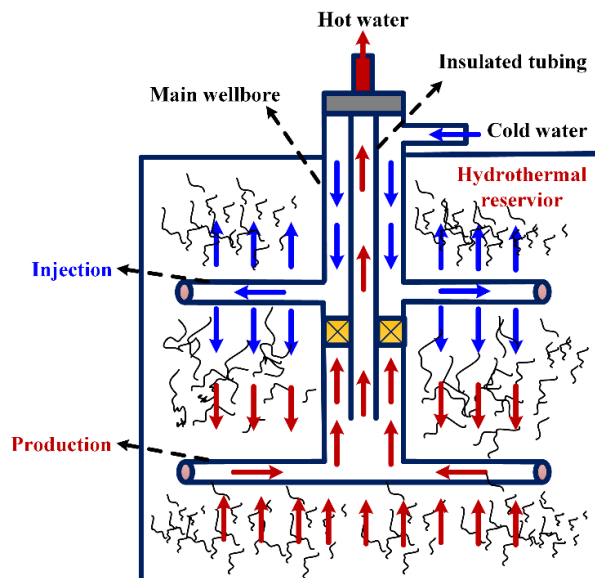


Figure 1: Schematic of hydrothermal extraction for novel two-layer multilateral horizontal wells

This paper introduces a novel two-layer multilateral horizontal well system to explore hydrothermal geothermal resources efficiently. The schematic of the novel method is showed in Figure 1. One main wellbore is drilled to hydrothermal reservoir. Subsequently, a radial jet drilling (RJD) technology or micro hole coiled-tubing (CT) drilling technology is employed to side-track several multilateral horizontal wells from the main wellbore at the upper and lower formation. Finally, an insulated tubing is installed in the main wellbore and the annulus between the tubing and wellbore is sealed by a packer. The working fluid is injected from the annulus and injection wells into the hydrothermal reservoir, where it extracts heat from porous rocks and natural underground water. Afterwards, the working fluid is produced from the production wells and returns to the surface for electricity generation through the insulated tubing. The technology increases connectivity between wells and reservoirs. The injection capacity and productivity of hydrothermal systems will achieve huge growth. In addition, the technology can also reduce the number of wells and significantly cut down engineering construction costs. In general, a new way is provided for the economic and efficient development of geothermal resources. The application of the multilateral well technology has been mainly in the oil and gas industry while there are few reports on the application of multilateral well technology in the geothermal field. In December 2008, in a geothermal injection well in Klaipeda, Lithuania, 12 horizontal wellbores with a length of approximately 40 m were drilled sideways using radial horizontal well technology. Production data shows that the injection volume of the well has increased by 14% after the operation (Nair et al., 2017). The field practice shows the feasibility and good prospects of the application of multilateral well technology in geothermal fields.

The hydrothermal energy extraction involves heat transfer, water seepage, solid deformation and geochemical reactions which are coupled as a thermal-hydro-mechanical-chemical (THMC) process (Xu et al., 2015). It plays a crucial role to investigate the multiphase coupling process in reservoir to reveal the mechanism of heat extraction, predict the performance in porous media as well as service-life for stable utilization period. These multi-physical processes are complex and are affected by a large number of parameters. Therefore, the numerical method has been recognized as an available and useful approach to model and analyze the coupling process in hydrothermal reservoir (McDermott et al., 2006).

Scholars have established a mass of numerical simulation models to study the geothermal development process based on theories like heat transfer theory, fluid mechanics, seepage mechanics, elastic mechanics and so on. Luo et al. (2014) analyzed the effects of multiple parameters like injection rate, the permeability of fractures, the well perforation placement on a doublet CO₂-EGS system coupling the CO₂ flow and the heat transfer between the wellbores and the surrounding reservoir. Jiang et al. (2014) present a 3D triplet well EGS model which is capable of simulating the complete subsurface thermo-hydraulic process during EGS heat extraction, not only the thermo-flow in the reservoir and well boreholes, but also the heat conduction or transport in rocks enclosing the reservoir. Huang et al. (2017) establish an equation relating EGS heat extraction to reservoir heterogeneity based on a large number of cases with various heterogeneous reservoirs coupling fluid seepage flow and the heat extraction between two straight wells. Cheng et al. (2016) develop a three-dimensional thermal-hydrologic model considering water losses to simulate heat extraction from a doublet well EGS. Wu et al. (2016) considered heat extraction from a multiple fracture system with dipole wells and found optimal values for the number of fractures and fracture spacing. Shaik et al. (2011) investigates the role of heat transfer between the rock matrix and circulating fluid on economic hot water production from fractured geothermal systems and conclude that heat transfer between rock and fluid and fracture connectivity has a profound effect on the economic potential of a geothermal reservoir. Zeng et al. (2013) numerically investigate heat production potential from hot dry rock by water circulating through two horizontal wells based on the geological data at Desert Peak geothermal field and obtain desirable heat production performance under suitable conditions. Taron et al. (2009) introduce a method to couple the THMC capabilities of TOUGHREACT with the mechanical (M) framework of FLAC3D to examine THMC processes in deformable, fractured porous media and find that permeability and porosity are modified as fracture apertures dilate or contract under the influence of pressure solution, thermal-hydro-mechanical compaction/dilation, and mineral precipitation/dissolution.

However, previous researchers have made many simulations on HDR geothermal system and most of them are based on two-well systems. At present, there is a lack of comprehensive and through analysis on the heat extraction performance of the novel heat extraction system especially on hydrothermal geothermal reservoirs. In this paper, a novel method is proposed to exploit hydrothermal system with two-layer multilateral horizontal wells. Considering the local thermal equilibrium theory, a three-dimensional porous medium unsteady flow and heat transfer coupling model is established and the model has been verified by Pandey et al. (2017). The novel model involves hydrothermal reservoirs (filled with random fractures), multilateral horizontal injection wells and production wells. The numerical solution of the model is implemented in the commercial finite element software, COMSOL Metaphysics. Four typical parameters, average production temperature, average pressure on injection wells, average production rate, and net heat power, are defined and analyzed to evaluate the extraction performance of the geothermal system. The pressure field, velocity field and reservoir temperature field at different times are compared and investigated to describe visually the dynamic change trend of the hydrothermal system.

2. MODEL DESCRIPTION

This paper proposes an idealised model for exploiting hydrothermal reservoirs with two-layer multilateral horizontal wells. The novel hydrothermal system contains a hydrothermal reservoir, a main wellbore, injection wells with four horizontal lateral wellbores, and production wells also with four lateral wellbores parallel to the injection wells. A schematic diagram is shown in Figure 1.

2.1 Model Assumptions

The hydrothermal geothermal reservoir is dual matrix involving both porous medium and natural fractures. However, the distribution of natural cracks is difficult to obtain. It is beyond the scope of the research that positions and shapes of the cracks are accurately depicted. Therefore, the hydrothermal reservoir is equivalently regarded as a single porous medium, and the values of permeability, porosity and other parameters are the same as reservoir actual parameters. The dynamic trend of production in the single porous reservoir is consistent with that in a dual matrix.

The basic assumptions of the model are as follows: (1) by simplification, the geothermal reservoir is a homogeneous, isotropic continuous medium; (2) local thermal equilibrium between solid and fluid is described and there is no temperature difference between fluid and reservoir matrix; (3) no flow on the top of the reservoir due to the extremely low permeability of the cap compared with high permeable formation; (4) water is in liquid phase under the model conditions (pressure is 20-40 MPa, temperature is 400 K to 500 K). Therefore, the reservoir is always in single-phase flow. Heat transfer between the liquid and the porous medium follows the theory of heat transfer in porous media. The seepage of the fluid conforms to Darcy's law. (5) There is no chemical reaction between the injected working fluid and the reservoir as hot water from production wells recharges to injection wells after power generation. (6) The reservoir depth is shallow, and the production fluid is reinjected. Therefore, the rock deformation is not considered because the formation pressure drops slowly.

2.2 The Governing Equations

The mass conservation equation of fluid flowing in the porous media is formulated as follows:

$$\frac{\partial(\rho_f \varphi)}{\partial t} + \nabla \cdot (\rho_f u) = -Q_f \quad (1)$$

where ρ_f (kg/m³) indicates the density of water, φ represents the porosity of the reservoir. t (s) is time, u (m/s) is Darcy velocity, and Q_f (kg/s) represents mass flow rate in a porous medium. According to Darcy's law, u (m/s) can be expressed by the following equation:

$$u = -\frac{k}{\mu_f} (\nabla p + \rho_f g \nabla z) \quad (2)$$

where k (m²) represents the reservoir permeability, μ_f (Pa·s) represents the viscosity of water, p (Pa) represents pressure, $\rho_f g \nabla z$ represents the gravity term, and z indicates the vertical direction.

In this paper, the local thermal equilibrium is applied to describe the heat transfer process between the working fluid and the reservoir rock which means there is no temperature difference between the fluid and rock. The heat transfer process in porous media is described by the following energy equation:

$$(\rho c_p)_{eff} \frac{\partial T}{\partial t} + \rho_f c_{p,f} u \cdot \nabla T - \nabla \cdot (\lambda_{eff} \nabla T) = -Q_{f,E} \quad (3)$$

where T (K) indicates the temperature of the porous medium, $c_{p,f}$ (J/(kg·K)) is the heat capacity of the working liquid, and $Q_{f,E}$ (W/m³) is the heat flow rate in the porous medium. $(\rho c_p)_{eff}$ and λ_{eff} respectively represent the effective volumetric heat capacity and effective thermal conductivity, which are defined by a volume averaging model to account for both reservoir rock and geothermal fluid properties.

$$(\rho c_p)_{eff} = (1 - \varphi) \rho_s + \varphi \rho_f c_{p,f} \quad (4)$$

$$\lambda_{eff} = (1 - \varphi) \lambda_s + \varphi \lambda_f \quad (5)$$

where ρ_s (kg/m³) is the reservoir rock density, $c_{p,s}$ (J/(kg·K)) is the reservoir rock heat capacity, and λ_s (W/(m·K)) is the thermal conductivity of the reservoir rock.

The physical properties of water vary with temperature. The density ρ and viscosity μ are both functions of temperature.

$$\rho = \begin{cases} 1000 \times \left(1 - \frac{(T_c - 3.98)^2}{503570} \times \frac{T_c + 283}{T_c + 67.26} \right) & 0^\circ\text{C} \leq T_c \leq 20^\circ\text{C} \\ 996.9 \times \left(1 - 3.17 \times 10^{-4} \times (T_c - 25) - 2.56 \times 10^{-6} \times (T_c - 25)^2 \right) & 20^\circ\text{C} \leq T_c \leq 250^\circ\text{C} \\ 1758.4 + 10^3 T (-4.8434 \times 10^{-3} + T(1.0907 \times 10^{-5} - T \times 9.8467 \times 10^{-9})) & 250^\circ\text{C} \leq T_c \leq 300^\circ\text{C} \end{cases} \quad (6)$$

where ρ (kg/m³) indicates the water density, T_c (°C) indicates Celsius temperature, and T (K) indicates Kelvin temperature.

$$\mu = \begin{cases} 1.787 \times 10^{-3} \times e^{(T_c \times (-0.033 + 1.962 \times 10^{-4} \times T_c))} & 0^\circ\text{C} \leq T_c \leq 40^\circ\text{C} \\ 10^{-3} \times (1 + 1.5512 \times 10^{-3} \times T_c)^{-1.572} & 40^\circ\text{C} \leq T_c \leq 100^\circ\text{C} \\ 0.2414 \times 10^{\frac{247.8}{T-140}} \times 10^{-4} & 100^\circ\text{C} \leq T_c \leq 300^\circ\text{C} \end{cases} \quad (7)$$

where μ (Pa·s) indicates water viscosity.

2.3 Coupling and Validation

Darcy's law controls the flow field. It can be seen from Equation (2) that the variables describing Darcy's law mainly include fluid velocity, pressure gradient, and fluid properties. The theory of heat transfer in porous media controls the heat transfer field of a fluid. It can be seen from its theoretical Equation (3) that the variables describing the heat transfer field are physical properties such as temperature, fluid velocity and heat capacity. When the reservoir temperature T varies, the heat transfer field is directly affected. The influence of temperature on the density and viscosity of the fluid cannot be neglected with the heat flow Q and temperature T changed, which indirectly affects the flow of the reservoir fluid. With the velocity of the fluid changing, it is worth noting that the heat transfer Equation (3) in the porous medium contains the velocity term u . That is, the fluid flow itself is accompanied by the convective heat. The flow field in turn affects the temperature field. In a word, this is completely a coupling process between hydraulics and heat transfer, which is TH coupling. The TH coupling numerical model has been proved to be reliable by Pandey et al. (2017) and can be used to describe the heat extraction process of the hydrothermal system with multilateral wells.

3. AN IDEAL EXTRACTION CASE WITH TWO-LAYER MULTILATERAL HORIZONTAL WELLS

3.1 Computation Model

This is a novel heat extraction model with two-layer multilateral horizontal wells. The model computational domains include: a hydrothermal geothermal reservoir, four lateral injection wells and four lateral production wells, as showed in Figure 2. The injection wells at the upside are parallel to the production wells at the lower side of the reservoir domain. The vertical depth of the calculation domain is 2500-3400 m, and the dimension of the domain is 1000 m × 1000 m × 900 m which is large enough to neglect the impact from the boundary. Each lateral well length is 100 m and the wellbore diameter is 0.05 m. The angle between two adjacent wells is 90°. The upper injection wells and the lower production wells are exactly opposite with well spacing 400m. The intersection of the multilateral wells is located at the center of the cross section of the well. The distance from the injection lateral wells to the top boundary of the reservoir is 300 m, and the distance from the production lateral wells to the bottom of the hydrothermal reservoir is 200 m. Geometric parameters of the reservoir are listed in Table 1.

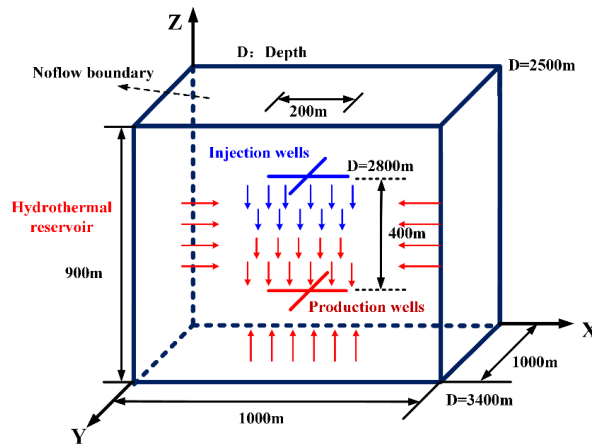


Fig. 2 Schematic of the model computation domain

As stated in Section 2.1, the hydrothermal reservoir is assumed to be an isotropic and homogeneous reservoir due to a heavy amount of work to describe precisely the positions and quantities of fractures. The complex dual medium is simplified into a single medium whose permeability, porosity, heat capacity and thermal conductivity of the reservoir are adapted from actual hydrothermal reservoirs. The main geometric parameters and reservoir physical properties are listed in Table 2.

Table 1 Geometrical parameters of the computational model

Parameters	Values
Hydrothermal reservoir	1000 m×1000 m×900 m
Horizontal well diameter	0.05 m
Horizontal well length	100 m
Injection and production well spacing	400 m
Distance from injection to reservoir top boundary	300 m

Table 2 Reservoir properties of the computational model

Physical properties	Hydrothermal reservoir
Density (kg/m ³)	2700
Heat conductivity(W/(m • K))	2.8
Heat capacity (J/(kg • K))	1000
Porosity (%)	10
Permeability (md)	8

3.2 Initial and Boundary Conditions

The initial temperature of the reservoir increases linearly from the top boundary to the bottom boundary with a temperature gradient of 0.04 K/m. The temperature at the top of the reservoir is 453.15 K while the bottom temperature is 489.15 K. In the initial state, the reservoir is saturated with groundwater. The original formation pressure also increases linearly from top to bottom with a pressure gradient of 8500 Pa/m. The top pressure of the reservoir is set as 25 MPa while the pressure at the bottom boundary is 32.65 MPa. The fixed injection input and constant pressure at the production wells should be applied in actual geothermal system. It is necessary to select the appropriate input and production pressure. Therefore, the total input is implemented as 80 kg/s which means 20 kg/s for each injection well to meet the economic development in current geothermal system. The production pressure is 28 MPa which is lower than the formation pressure at the production well location by 2 to 20 MPa. Besides, the temperature of the injection working liquid is set as 293.15 K equals to the surface temperature.

As assumed in Section 2.1, the top boundary of the hydrothermal system reservoir is a no-flow and constant temperature boundary. Besides, the four side boundaries and the bottom of the reservoir are implemented as constant pressure and temperature boundaries. It will take a long time for pressure and temperature fluctuations to reach the reservoir boundaries as the middle formation is the main area to be exploited. The energy beyond the computation domain can be constantly supplied to the hydrothermal reservoir. In general, the boundary temperature and pressure are always at initial temperature and pressure. The main initial and boundary conditions are shown in Table 3.

Table 3 Parameters of the initial and boundary conditions

Parameters	Values
Temperature gradient	0.04 K/m
Pressure gradient	8500 Pa/m
Temperature at the top boundary	453.15 K
Pressure at the top boundary	25 MPa
Injection mass flow rate	80 kg/s
Pressure at the production wells	28 MPa
Injection temperature	293.15 K

3.3 Simulation Mesh

A schematic diagram of the mesh division of the two-layer multilateral well hydrothermal geothermal system is shown in Figure 3. The most frequent fluid flow and heat exchange are between the wells and the reservoir. The reservoir between the injection wells and the production wells is the most concerned part. Considering the computational efficiency and computer internal storage, the

hydrothermal reservoir is divided into three parts when meshing from the top face to the bottom face of the formation: $1000\text{ m} \times 1000\text{ m} \times 300\text{ m}$, a hexahedron from the upper boundary to the first layer; $1000\text{ m} \times 1000\text{ m} \times 400\text{ m}$, with extremely fine meshes in a $700\text{ m} \times 700\text{ m} \times 400\text{ m}$ cube in the center from the horizontal injection wells to production wells; $1000\text{ m} \times 1000\text{ m} \times 200\text{ m}$, a cube from the second layer multilateral production wells to the bottom of the reservoir. Furthermore, the longitudinal mesh division affects the simulation accuracy. The depth is divided into 70 layers, and the average spacing of the vertical grid is 12.9 meters. In general, the grid of the entire model contains 176,260 units and the degree of freedom of solution is 1207141 (extra 297,444 internal degrees of freedom).

The partial differential equations are calculated by the separation method in the commercial finite element software COMSOL. The heat extraction period is 30 years. The time step for the first 10 days is 0.5 days and the time step from the 12th day to the 30th day is 2 days. When geothermal reservoir is exploited from the 35th day to the 365th day, the time step is 5 days. The time step is 60 days from the 365th day to the 30th year.

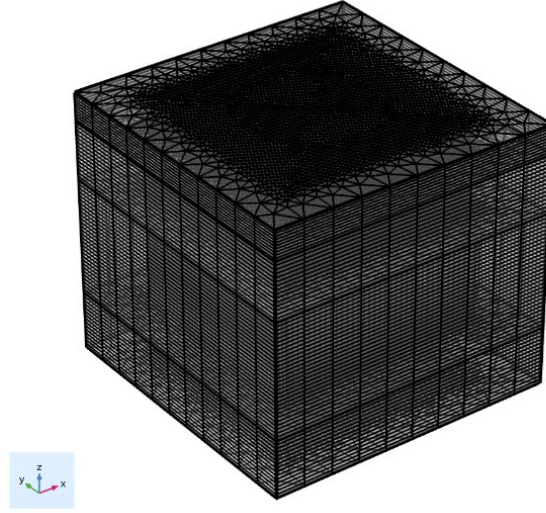


Fig. 3 Numerical meshing schemes of hydrothermal reservoirs

3.4 Evaluation System of Heat Extraction Performance

Four parameters for the thermal performance of the hydrothermal geothermal system are defined to facilitate the analyses: average production temperature, average pressure at injection wells, production rate and net heat power.

3.4.1 Average Production Temperature

The average production temperature (T_{out}) of the production wells is defined by:

$$T_{out} = \frac{\int_L T(t,l)dl}{L} \quad (8)$$

where L (m) indicates the total length of the multilateral production wells and $T(t,l)$ (K) is the temperature of production wells at the time t (s) and the location l (m).

The temperature drop of production wells should be as low as possible to achieve stable development of hydrothermal geothermal systems. Although geothermal energy is a clean and renewable energy, there may be a lag in energy recharge. It takes time for the geothermal system to return to the original state because the heat in the surrounding formation cannot be transferred to the target area in time. Consequently, it is necessary to stop production when the temperature drop of the production well in the geothermal system exceeds $10\text{ }^{\circ}\text{C}$ (Tester et al., 2007).

T_{out} can evaluate the production performance directly. The efficient system is that T_{out} is stable for a long time within the maximum temperature drop limits.

3.4.2 Average Injection Pressure

The average injection pressure p_{in} represents the average pressure at the location of the multilateral injection well, which is given by:

$$p_{in} = \frac{\int_L p(t,l)dl}{L} \quad (9)$$

L (m) indicates the length of the multi-branch injection well, and $p(t,l)$ (Pa) indicates the pressure of injection wells at the time t (s) and the location l (m).

p_{in} is a critical parameter for evaluating the rationality of system. Cold water is injected into the formation and hot water is produced from the production wells for power generation. The injection pressure will vary during the geothermal process. The injection pressure cannot exceed the formation fracture pressure which may eventually cause damage to formation.

3.4.3 Production Rate

Production rate Q_{out} is the average mass flow rate per unit length of the injection well. The equation Q_{out} is given by:

$$Q_{out} = \frac{\int_L q(t, l) dl}{L} \quad (10)$$

where L (m) indicates the length of the multilateral production well, and $q(t, l)$ (kg/(s·m)) indicates the mass flow rate per unit length of the injection well the time t (s) and the location l (m).

Q_{out} is a direct manifestation of the production performance. The larger the output rate, the more energy the liquid carries indicating better extraction effect.

3.4.4 Net Heat Power

The net heat power P_{net} is the difference between the production thermal power P_{out} and injection thermal power P_{in} . The definitions are shown as follows:

$$P_{net} = P_{out} - P_{in} \quad (11)$$

$$P_{out} = \frac{\int_L c_{p,f} q(t, l) T(t, l) dl}{L} \quad (12)$$

$$P_{in} = c_{p,f} Q_{in} T_{in} \quad (13)$$

where $c_{p,f}$ (J/(kg·K)) is the heat capacity of the working fluid. T_{in} (K) and Q_{in} (kg/s) represent the temperature of the injection liquid and the input mass flow rate, respectively.

P_{net} characterizes geothermal system performance and describes the net energy extracted from the formation per unit time. The larger the P_{net} is expected within the limits of production temperature drop.

In summary, T_{out} and p_{in} are used to reflect whether the system is reasonable. Besides, T_{out} , Q_{out} and P_{net} are used to evaluate the production performance. It is worth noting that all four parameters are functions of time t (s).

4. RESULTS AND DISCUSSIONS

The appropriate initial and boundary parameters are input to COMSOL to calculate the characteristic parameters as defined in Section 3.4. The injection temperature is 293.15 K. The total injection mass flow is 80 kg/s, which means the injection flow rate for every lateral well is 0.5 kg/(m·s) and the pressure on the production wells is 28 MPa. Four parameters evolution T_{out} , p_{in} , Q_{out} and P_{net} with time are drew to evaluate the effect of the system.

4.1 Evaluation of Characteristic Parameters

Figure 4 indicates evolution of production temperature T_{out} and injection pressure p_{in} with time. The solid red line corresponding to the left y-axis represents T_{out} while the blue dashed line corresponding to the right y-axis is p_{in} . During the 30-year cycling, T_{out} tends to decrease overall. The formation near the injection well heats the cold working fluid, and the hot water is discharged near the production well. Consequently, the reservoir energy is consumed gradually. Moreover, according to the falling range of the temperature at the production well, geothermal development can be divided into two phases: the stable production phase and reduction phase. The temperature drop in the first phase is small and the trend is a straight line with a slope approaching zero around 480K.

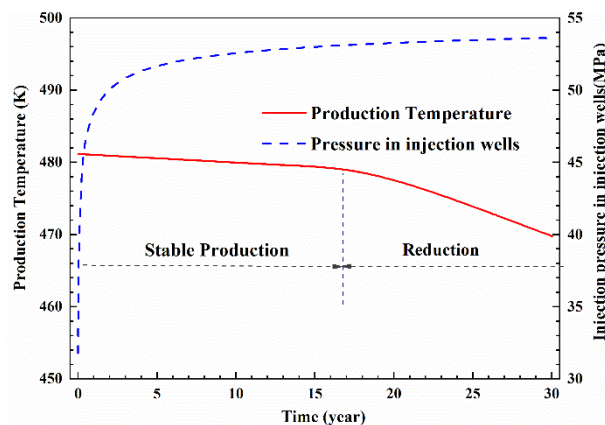


Fig. 4 Evolution of production temperature T_{out} and injection pressure p_{in} with time

This is because the temperature fluctuation near the injection wells has not yet propagated to the production wells. The stable production lasts for a long time of 17 years. When the temperature fluctuation is transmitted to the production wells, the reservoir near the production well needs to replenish energy for the low temperature zone. Therefore, the temperature drop of the production wells is large and shows a linear change in the reduction phase. Finally, the temperature drops to 470K at the end of the simulated period of 30 years which is 11K lower than the initial temperature. The reduction phase is 13 years. Actually, the purpose of geothermal development is to extend the period of the stable production phase under operation constraints and reservoir conditions. Extending the stable production can be achieved by adjusting the operation parameters or the well type.

The blue curve indicates the pressure p_{in} at the underground injection wells. It can be seen from Figure 4 that p_{in} increases greatly from 31 MPa to 46 MPa in the previous 3 years. Because the temperature of the injection well drops from 483.15 to 293.15 K in a short time when the cold fluid is injected. Figure 5 shows the water viscosity variation with temperature. The flow resistance increases by 7 times with sharp drop of temperature at the injection wells as can be seen from Figure 5. According to Darcy's law, the pressure difference is the power of the fluid flow. It is necessary to increase the p_{in} to balance the rapid flow resistance when the flow rate is constant. The viscosity of the fluid varies slowly with small temperature variation around injection wells after 3-years extraction. As a result, the corresponding injection pressure liquid increases slowly. The temperature around the injection wells finally equals to 293.15K and the injection pressure tends to be the maximum pressure that is not more than 55 MPa. It is worth noting that the underground injection pressure cannot exceed the formation fracture pressure and the formation leakage pressure. It is necessary to install the casing to seal the formation and the horizontal wellbore to prevent thermal reservoir damage.

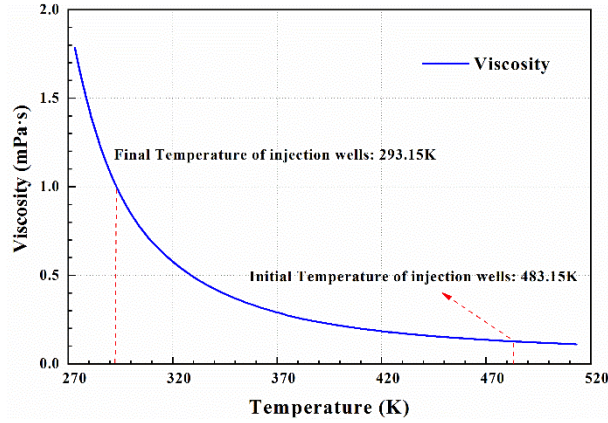


Fig. 5 Water viscosity variation with temperature

Figure 6 is the evolution of production rate and net heat power with time. The solid blue line is production rate Q_{out} corresponding to the left Y-axis while the red dashed line indicates net heating power P_{net} corresponding to the right Y-axis. It can be seen from the figure that the trend of Q_{out} and P_{net} is consistent, which confirms to the definition of P_{net} . Furthermore, the turning point of the two curves from the stable production phase to the reduction phase are 0-17 years and 17-30 years respectively which agrees with the previous discussion.

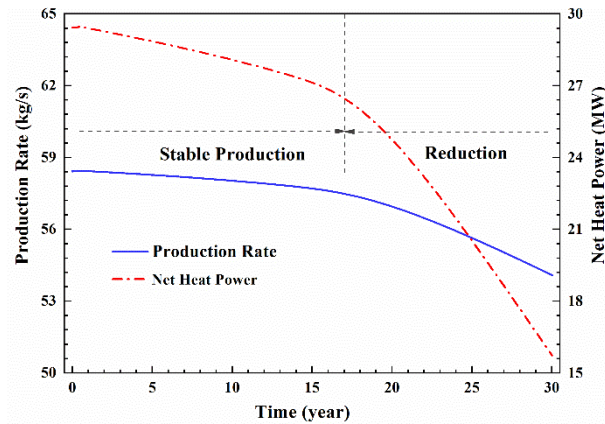


Fig. 6 Evolution of production rate Q_{out} and net heat power P_{net} with time

Q_{out} tends to decrease over time as a result of low pressure and low temperature. The low-pressure zone and the low temperature zone will gradually diffuse from the injection wells to the production wells with the development of the geothermal system. The low-pressure zone will lead to insufficient fluid flow, and the low temperature zone will increase the resistance of the fluid flow. During the stable production, the output is smooth because the low temperature zone and the low-pressure zone have not been completely transferred to the production well. The maximum output is 58.4 kg/s and the minimum yield is 57.5 kg/s in stable phase. However, the reduction phase begins when the low temperature zone and the low-pressure zone are transmitted to the production well. The two

curves both decline linearly. The minimum output is 54.5 kg/s and the injection rate is 80 kg/s on 30th year. Therefore, injection and production is underbalanced.

P_{net} decreases over time. In the stable production, the net heat power shows a linear downward trend with time, which is slightly larger than Q_{out} drop. The maximum net heat power is 29.5 MW while the minimum thermal power is 15.7 MW during the first phase. According to the definition of P_{net} , the main reason for the decrease of P_{net} is Q_{out} and T_{out} . Q_{out} is the main factor during the first stage as the temperature at the production well is stable at 480 K. Besides, P_{net} also showed a linear decline with time in the reduction stage, which is larger than the decline of Q_{out} in the decay phase. P_{net} of the system is 15.7 MW on 30th year. Q_{out} and T_{out} are greatly reduced so they both contribute to the decline of P_{net} .

4.2 Evaluation of the Flow and Temperature Fields

4.2.1 Distribution of the Flow and Temperature around the Wells

Figure 7 is a combination of temperature contours, pressure contours and velocity contours on the 5th, 10th, 20th and 30th year of hydrothermal reservoir production respectively. The upper and lower surfaces of each contour map are the plane where the injection well and the production well are located with the dimension is 700 m \times 700 m. The inclined plane in the middle indicates the internal variation of the reservoir.

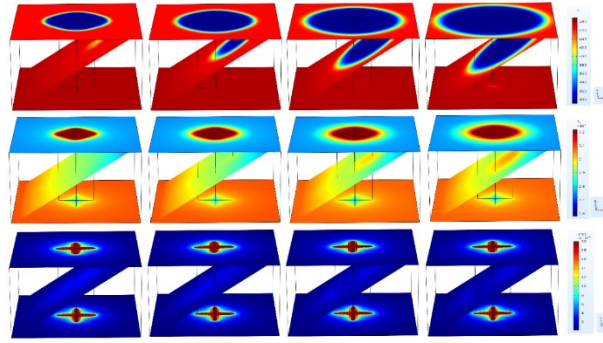


Fig. 7 Temperature contours (first row), pressure contours (second row), and velocity contours (third row) in the reservoir on the 5th, 10th, 20th and 30th year (from left to right) respectively

The first row in the figure represents the contour map of the temperature at different times. It can be seen from the figure that in the first five years, the temperature near the injection well is the lowest and the low temperature area has not spread widely during the first 5-years extraction. As cycling proceeds, the low temperature zone is centered on the injection wellbores and spreads uniformly around the reservoir in the horizontal direction. As shown in the vertical direction, temperature fluctuation extends from the upper injection wells to the production wells below. The temperature drop propagates to the reservoir after 10-years development. By the 30th year, at the level of the injection well, the low temperature zone has spread to 350 m horizontally and has expanded to the production well vertically.

The second row represents the contour map of the pressure at different times. It can be seen from the figure that the highest pressure appears at the injection wells and the lowest pressure occurs at the production well. The flow resistance near the production wells is much smaller than that near the injection well because of large temperature difference between two areas. As the extraction continues, the injection pressure expands gradually from the injection wells to the surrounding reservoirs. Besides, the high pressure region appears like a circle in the plane of injection wells while the low-pressure area changes a little around the production wells.

The third row represents velocity contour map at different times. It can be seen from the figure that the largest flow velocity occurs near the injection wells and the production wells while the flow speed is relatively small in blue regions. Also, the velocity distribution is gradually stable without significant fluctuations.

4.2.2 Distribution of the Flow and Temperature in the Reservoir

Figure 8 shows the evolution of heat recovery efficiency at different times of 5th, 10th, 20th and 30th year. This is a reservoir space of 700 m \times 700 m \times 400 m between injection wells and production wells. Actually the recovery map can describe the diffusion of low temperature zone directly from the injection wells to the surrounding reservoirs. The extended area is shaped like a funnel as the vertical temperature propagates faster than the lateral direction due to the gravity. The temperature propagation front has a spurt phenomenon near the production well because of the large fluid flow rate at the production wells. The low temperature region accounts for 1/3 of the reservoir volume with a high value of recovery on 30th year.

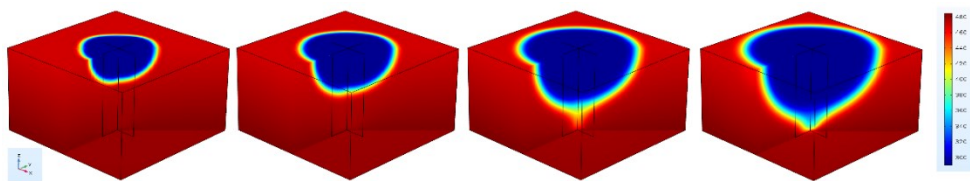


Fig. 8 Reservoir recovery on the 5th, 10th, 20th and 30th year (from left to right) respectively

Figure 9 shows the pressure distribution cloud map at different times, which shows the pressure change of formation during thermal extraction more intuitively. The high-pressure zone centered on the injection position is shaped like a sphere and gradually becomes

larger as the mining proceeds. On the contrary the low pressure zone centered on the production well is small and is limited to the production position. As a result, the overall pressure of the reservoir has become larger according to the color distribution during 30 years.

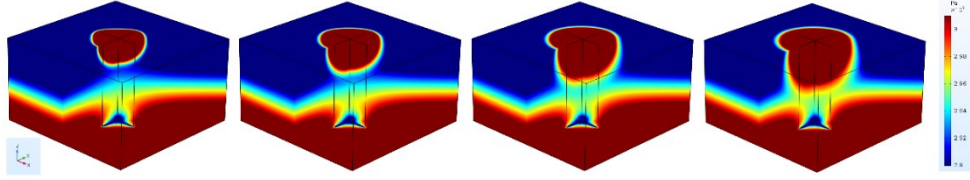


Fig. 9 Distribution of reservoir pressure on the 5th, 10th, 20th and 30th year (from left to right) respectively

Figure 10 shows the reservoir streamlines on the 30th year. Black arrows are streamlines. The red area is the high pressure area while the light area is the low pressure area. The fluid flows from the dark area to the light color area. As shown in Figure 10 the streamline arrow diverges outward from the injection wells and merges into the production wells. Besides, the flow line is perpendicular to the pressure contour.

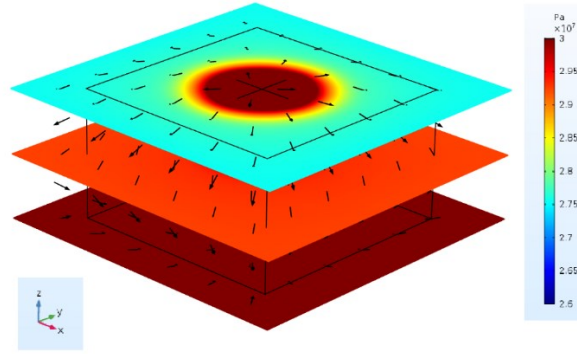


Fig. 10 Distribution of reservoir streamlines between injection and production wells on the 30th year

4. CONCLUSIONS

In this paper, two-layer multilateral horizontal wells are proposed to extract heat from hydrothermal geothermal system. Cold water enters the formation from the injection wells, and hot water is produced from the production wells for power generation. In this paper, only one main wellbore is drilled to complete the injection and production at the same time, which greatly reduces the cost of reservoir development. Moreover, the multilateral horizontal wells enhance the connectivity between the wellbore and the geothermal reservoir. Furthermore, the arrangement significantly improves the injection capacity and production capacity of the geothermal system. A three-dimensional unsteady fluid flow and heat transfer model is established for the two-layer multilateral horizontal well hydrothermal geothermal system. The numerical solution of the model was calculated by the finite element analysis software COMSOL. These simulation results depend on the model settings and model assumptions in this paper which may lead to different conclusions based on various settings and assumptions. The critical findings of this study as concluded as follows.

(1) Based on the model, four characteristic parameters are defined: average production temperature T_{out} , average pressure on injection wells p_{in} , average production rate Q_{out} , and net heat power P_{net} . The equation of physical properties of water is analyzed in detail combined with Darcy's law and the theory of heat transfer in porous media. Q_{out} and P_{net} are important characteristic parameters for evaluating production efficiency.

(2) T_{out} decreases with time overall during the heat extraction. The stable production stage and the reduction stage are defined according to the downtrend of T_{out} . By the way, p_{in} increases with time which is related to the propagation of the low temperature zone and the high pressure zone. The maximum injection pressure cannot exceed the formation fracture pressure. Casing should be installed in the horizontal injection wells to prevent fracturing and leakage. Q_{out} and P_{net} slowly decline with time in the stable production stage while the two parameters rapidly decrease with time in the reduction stage.

(3) The temperature contours, pressure contours and streamline contours of the system are analyzed to describe the production dynamics of the reservoir more intuitively. The temperature cloud map shows that the low temperature region of the reservoir expands from the injection wells with a funnel-like distribution. Therefore, the cold working fluid takes the heat near the injection wells. As a result, the average temperature of the production wells gradually decreases. The pressure cloud diagram shows that the high pressure region near the injection wells is spherical and gradually becomes larger with time. However, the low pressure region centered on the production well is limited to the periphery of the production well and changes a little with time. The streamline diagram shows that the working fluid flows from the injection well into the formation, and the production well extracts hot water from the underground reservoir.

(4) In this study, a two-layer multilateral horizontal well model is established to simulate the heat extraction performance of a hydrothermal system. It shows excellent performance within 30 years of extraction. However, a comparison case of the two-well system under the same conditions should be investigated. Moreover, the performance of multilateral horizontal well system is influenced by reservoir geological parameters, operation parameters and well parameters. In further work, parameter sensitivity should be analyzed to determine the effects of three kinds of parameters on the hydrothermal reservoir schemes. A productivity optimization equation should be established based on parameter sensitivity analysis.

ACKNOWLEDGMENTS

The authors would like to acknowledge the National Key Research and Development Program of China (Grant No. 2018YFB1501804) and National Natural Science Funds for Excellent Young Scholars of China (Grant No. 51822406). Furthermore, support from the Program of Introducing Talents of Discipline to Chinese Universities (111 Plan) (Grant NO. B17045) is appreciated.

REFERENCES

- Cao, W., Huang, W., & Jiang, F.: A novel thermal–hydraulic–mechanical model for the enhanced geothermal system heat extraction, *International Journal of Heat and Mass Transfer*, **100**, (2016), 661-671.
- Cheng, W. L., Wang, C. L., Nian, Y. L., Han, B. B., & Liu, J.: Analysis of influencing factors of heat extraction from enhanced geothermal systems considering water losses, *Energy*, **115**, (2016), 274-288.
- Gérard, A., Genter, A., Kohl, T., Lutz, P., Rose, P., & Rummel, F.: The deep EGS (Enhanced Geothermal System) project at Soultz-sous-Forêts (Alsace, France), *Geothermics*, **35**, (2006), 473-483.
- Han C. and Yu X.: Sensitivity analysis of a vertical geothermal heat pump system, *Applied Energy*, **170**, (2016), 148-160.
- Huang, W., Cao, W., & Jiang, F.: Heat extraction performance of EGS with heterogeneous reservoir: A numerical evaluation, *International Journal of Heat and Mass Transfer*, **108**, (2017), 645-657.
- Jiang, F., Chen, J., Huang, W., & Luo, L.: A three-dimensional transient model for EGS subsurface thermo-hydraulic process, *Energy*, **72**, (2014), 300-310.
- Jiyang, W., & Shaopeng, H.: Compilation of heat flow data in the China continental area. *Seismology and Geology*, **12**, (1990), 351-366.
- Lin W., Liu Z., Wang W., Wang G.: The assessment of geothermal resources potential of China, *Geology in China*, **40**, (2013), 312-321.
- Lukawski, M. Z., Silverman, R. L., & Tester, J. W.: Uncertainty analysis of geothermal well drilling and completion costs. *Geothermics*, **64**, (2016), 382-391.
- Luo, F., Xu, R. N., & Jiang, P. X.: Numerical investigation of fluid flow and heat transfer in a doublet enhanced geothermal system with CO₂ as the working fluid (CO₂-EGS), *Energy*, **64**, (2014), 307-322.
- McDermott, C. I., Randriamanjatoa, A. R., Tenzer, H., & Kolditz, O.: Simulation of heat extraction from crystalline rocks: the influence of coupled processes on differential reservoir cooling, *Geothermics*, **35**, (2006), 321-344.
- Nair R, Peters E, Šliaupa S, Valickas R, Petrauskas S.: A case study of radial jetting technology for enhancing geothermal energy systems at Klaipėda geothermal demonstration plant, 42nd workshop on Geothermal Reservoir Engineering, Stanford University, (2017), 1-11.
- Pandey, S. N., Chaudhuri, A., & Kelkar, S.: A coupled thermo-hydro-mechanical modeling of fracture aperture alteration and reservoir deformation during heat extraction from a geothermal reservoir, *Geothermics*, **65**, (2017), 17-31.
- Panel, M. L. I.: The future of geothermal energy-impact of enhanced geothermal systems (EGS) on the United States in the 21st century. Idaho National Laboratory, Idaho Falls, ID (2006).
- Shaik, A. R., Rahman, S. S., Tran, N. H., & Tran, T.: Numerical simulation of fluid-rock coupling heat transfer in naturally fractured geothermal system, *Applied thermal engineering*, **31**, (2011), 1600-1606.
- Shi Y, Song X., Li G., Yang R., Shen Z., Lyu Z.: Numerical investigation on the reservoir heat production capacity of a downhole heat exchanger geothermal system. *Geothermics*, **72**, (2018), 163-169.
- Sims, R. E. Renewable energy and climate change mitigation: an overview of the IPCC Special Report, *Springer, Weather matters for energy*, (2014), 91-110.
- Song X., Shi Y., Li G., Yang R., Wang G., Zheng R., Li J., Lyu Z.: Numerical simulation of heat extraction performance in enhanced geothermal system with multilateral wells, *Applied Energy*, **28**, (2018), 325-337.
- Taron, J., & Elsworth, D.: Thermal–hydrologic–mechanical–chemical processes in the evolution of engineered geothermal reservoirs, *International Journal of Rock Mechanics and Mining Sciences*, **46**, (2009), 855-864.
- Tester, J. W., Anderson, B. J., Batchelor, A. S., Blackwell, D. D., DiPippo, R., Drake, E. M., Garnish, J., Livesay, B., Moore, M. C., Nichols, K. & Petty, S.: Impact of enhanced geothermal systems on US energy supply in the twenty-first century. *Philosophical Transactions of the Royal Society A: Mathematical, Physical and Engineering Sciences*, **365**, (2007), 1057-1094.
- Wang, G. L., Zhang, W., Ma, F., Lin, W. J., Liang, J. Y., & Zhu, X.: Overview on hydrothermal and hot dry rock researches in China, *China Geology*, **1**, (2018), 273-285.

- Wu, B., Zhang, X., Jeffrey, R. G., Bunger, A. P., & Jia, S.: A simplified model for heat extraction by circulating fluid through a closed-loop multiple-fracture enhanced geothermal system, *Applied energy*, **183**, (2016), 1664-1681.
- Xu, R., Zhang, L., Zhang, F., & Jiang, P.: A review on heat transfer and energy conversion in the enhanced geothermal systems with water/CO₂ as working fluid. *International Journal of Energy Research*, **39**, (2015), 1722-1741.
- Zeng, Y. C., Su, Z., & Wu, N. Y.: Numerical simulation of heat production potential from hot dry rock by water circulating through two horizontal wells at Desert Peak geothermal field, *Energy*, **56**, (2013), 92-107.
- Zhang, Q., Chen, S., Tan, Z., Zhang, T., & Mclellan, B. Investment strategy of hydrothermal geothermal heating in China under policy, technology and geology uncertainties, *Journal of cleaner production*, **207**, (2019), 17-29.